



Naringin ameliorates obesity via stimulating adipose thermogenesis and browning, and modulating gut microbiota in diet-induced obese mice

Xiaoping Li^a, Zhao Yao^b, Xinyue Qi^c, JinLing Cui^a, Yuliang Zhou^c, Yihong Tan^c,
Xiaojun Huang^d, Hui Ye^{c,*}

^a College of Culinary Science, Sichuan Tourism University, Chengdu, 610100, China

^b School of Health Industry, Sichuan Tourism University, Chengdu, 610100, China

^c School of Chemistry, Chemical Engineering, and Biotechnology, Nanyang Technological University, Singapore, 637371

^d State Key Laboratory of Food Science and Resources, China-Canada Joint Lab of Food Science and Technology (Nanchang), Nanchang University, 235 Nanjing East Road, Nanchang, 330047, China

ARTICLE INFO

Handling Editor: Dr. Quancai Sun

Keywords:

Naringin
Obesity
Thermogenesis
Fat browning
Gut microbiota
Fecal metabolites

ABSTRACT

Naringin, a natural flavanone primarily found in citrus fruits, has garnered increased attention due to its recognized antioxidative, anti-inflammatory, and cardioprotective attributes. However, the functions of naringin in regulating energy expenditure are poorly understood. In the present study, we observed that twelve weeks of naringin supplementation substantially reshaped the metabolic profile of high-fat diet (HFD)-fed mice, by inhibiting body weight gain, reducing liver weight, and altering body compositions. Notably, naringin exhibited a remarkable capacity to augment whole-body energy expenditure of the tested mice by enhancing the thermogenic activity of brown adipose tissue (BAT) and stimulating browning of inguinal white adipose tissue (iWAT). Furthermore, our results showed naringin supplementation modified gut microbiota composition, specifically increasing the abundance of *Bifidobacterium* and *Lachnospiraceae_bacterium_28-4*, while reducing the abundance of *Lachnospiraceae_bacterium_DW59* and *Dubosiella_newyorkensis*. Subsequently, we also found naringin supplementation altered fecal metabolite profile, by significantly promoting the production of taurine, tyrosol, and thymol, which act as potent activators of thermoregulation. Interestingly, the metabolic effects of naringin were abolished upon gut microbiota depletion through antibiotic intervention, concurrently leading to the disappearance of naringin-induced thermogenesis and protective actions on diet-induced obesity. This discovery revealed a novel food-driven cross-sectional communication between gut bacteria and adipose tissues. Collectively, our data indicate that naringin supplementation stimulates BAT thermogenesis, alters fat distribution, promotes the browning process, and consequently inhibits body weight gain; importantly these metabolic effects require the participation of gut bacteria.

1. Introduction

Obesity, primarily caused by imbalance of energy intake and expenditure, is closely associated with hyperlipidemia, type 2 diabetes, and tumors (GBD 2015 Obesity Collaborators et al., 2017; Shin et al., 2013; Wang et al., 2020). Activation of the non-shivering thermogenic program in brown adipose tissue (BAT) and white adipose tissue (WAT) proves to be a promising method for increasing energy expenditure during the treatment of obesity [4]. In mammals, two developmentally distinct types of brown adipocytes exist; the classical or constitutive BAT that arises during embryogenesis, and the beige adipose tissue that is

recruited postnatally within WAT in the process called browning (Kurłowicz and Puzianowska-Kuznicka, 2020). BAT, which is rich in mitochondria and uncoupling protein 1 (UCP1), is characterized by the ability to promote non-shivering thermogenesis (Cohen and Kajimura, 2021; Fernández-Verdejo et al., 2019; MacLean et al., 2015). The activation of UCP1 leads to uncoupling electron transport from ATP synthesis and dissipates the proton gradient to generate heat (Y. Han et al., 2017; Wolfrum and Gerhart-Hines, 2022). Beige cells, intermediate between white and brown adipocytes, can be induced from white adipocytes in WAT by cold stimulation, exercise training, or β -adrenergic agonists (Cohen and Kajimura, 2021; Fernández-Verdejo et al., 2019;

* Corresponding author.

E-mail address: ye.hui@ntu.edu.sg (H. Ye).

<https://doi.org/10.1016/j.crfs.2024.100683>

Received 28 October 2023; Received in revised form 7 December 2023; Accepted 17 January 2024

Available online 18 January 2024

2665-9271/© 2024 The Authors. Published by Elsevier B.V. This is an open access article under the CC BY-NC-ND license (<http://creativecommons.org/licenses/by-nc-nd/4.0/>).

MacLean et al., 2015). Both beige and brown cells possess the capacity for thermogenesis as well as improvement of lipid and glucose metabolism (Wolfrum and Gerhart-Hines, 2022). Therefore, exploring a safe and effective agonist to activate UCP1 in brown and beige cells is a potential intervention strategy for compacting obesity and related metabolic disease.

Naringin is a flavanone-7-O-glycoside, primarily isolated from citrus fruits, such as grapefruit [9], and naringin has been reported for its antihyperlipidemic, antioxidant, anti-inflammatory and anti-hyperglycemic functionalities (Chen et al., 2016; Y. Han et al., 2017). A few isolated literature reports have suggested that naringin could prevent obesity, but the corresponding underlying mechanism for its weight-control effect is not well understood (Alam et al., 2013; Sui et al., 2018). Indeed, Lee et al. reported that naringin upregulated the expression level of UCP1 gene in 3T3-L1 cells, a common *in vitro* model of white adipocyte. Nevertheless, naringin whether induces thermogenesis in mammals still requires further investigation.

Interestingly, microbial communities of the gut are known to have an influence on the energy balance, nutrient harvesting, fat accumulation, and inflammation responses of the host's body (Moreno-Navarrete and Fernandez-Real, 2019; Ussar et al., 2015). In addition, alteration of gut microbiota community is closely related to the expression levels of thermogenic genes in adipose tissue (Moreno-Navarrete and Fernandez-Real, 2019). In microbiota depletion model and in germ-free model, thermogenic capacity in mice was dramatically decreased, and accompanied with downregulation of UCP1 expression and reduction of the browning process of WAT (B. Li et al., 2019). In line with this, evidence suggests that increasing the activity of BAT is tightly associated with changing the composition of gut microbiota, contributing to the efficacy of weight-loss (Guo et al., 2019; G. Li et al., 2017). Importantly, previous works have demonstrated that polyphenol-rich fruit extracts ameliorate obesity and consequent metabolic disorders, and this is highly associated with the changes in the gut microbiota and bacterial metabolites (Anhê et al., 2015; Roopchand et al., 2015; Yang et al., 2022). Collectively, these suggested a potential mediating role of gut microbiota and their metabolites in the regulation of naringin in whole body thermogenesis.

In this study, we sought to explore the regulatory roles of naringin in body weight gain, adipocyte thermogenesis and intestinal microbiota composition in high-fat diet (HFD)-fed mice. We also examined the effects of naringin on the fecal metabolic profiles in obese mice. Furthermore, the role of the gut microbiota in mediating the effects of naringin on obesity were investigated using a pseudo sterile mouse model. These findings help us understand the weight control effect of naringin and provide a basis for the beneficial effect of citrus fruit consumption.

2. Methods

2.1. Reagents and materials

Naringin was obtained from Wuhan Xinxin Biotechnology Co., Ltd. (Wuhan, China) with a purity of $\geq 98\%$. Antibodies for β -actin, UCP1, and peroxisome proliferator-activated receptor gamma coactivator-1 alpha (PGC-1 α) were obtained from Abcam (Miami, USA). A high-fat diet (HFD, 46% of calories derived from fat) and a low-fat diet (LFD, 10% of calories derived from fat) were obtained from Research Diets Inc. (New Jersey, USA).

2.2. Animal studies

Six-week-old C57BL/6J male mice (weighted 22.1–23.5 g) were purchased from Nanjing Junke Bioengineering Co., Ltd. (Nanjing, China). All animals were housed in a room with a controlled environment (Temperature: 22 ± 2 °C, humidity 40–50%, 12-h light/dark cycle) and had free access to water and food during a one-week

acclimation period.

Thirty C57BL/6J mice were randomly divided into three groups (10 per group): (1) low-fat diet group (LFD); (2) a solvent-treated high-fat diet group (HFD) and (3) a 100 mg/kg/day naringin-treated HFD group (HFD-naringin). Naringin was suspended in 0.5% (w/v) sodium carboxymethyl-cellulose (CMC) solution as reported previously, and the mice received either CMC (LFD and HFD) or 100 mg/kg naringin by oral gavage for 12 weeks, and the dosages of naringin were based on a previous report (Kumar & Kumar, 2010; Sui et al., 2018). All experimental diets were stored at 4 °C and changed every 3 days. The mice body weight was monitored every week. For gut microbiota depletion treatment, twenty C57BL/6J male mice were administered with broad-spectrum antibiotics mix (bacitracin, neomycin, and streptomycin) in sterilized drinking water at 0.1% (w/v) of each drug, along with CMC (HFD-Abs) or 100 mg/kg naringin (HFD-naringin-Abs) daily for 10 weeks, body weights were measured weekly (Y. Liu et al., 2022).

At the end of the diet intervention, all mice were anesthetized, and blood was collected via cardiac puncture and centrifuged at $2000 \times g$ for 10 min at 4 °C in anticoagulant-coated tubes for further use. The brown adipose tissue (BAT), inguinal white adipose tissue (iWAT), epididymal white adipose tissue (eWAT) and liver tissues were removed, weighed, and stored at -80 °C.

2.3. Biochemical analysis

Plasma triglyceride (TG), total cholesterol (TC), low-density lipoprotein cholesterol (LDL-C), and high-density lipoprotein cholesterol (HDL-C) levels were detected by commercial kits of Jiancheng Co., Ltd (Nanjing, China). Glucose concentration was checked after fasting overnight using a portable glucose meter (Sinocare Inc., Changsha, China).

2.4. Glucose tolerance test

For GTT, mice were fasted for 16 h, following with oral gavage of glucose (1 g/kg), then, blood samples were collected from the tail at 0, 15, 30, 60, 90, and 120 min to measure the blood glucose concentrations.

2.5. Metabolic cages and core body temperature measurement

At week 10, mice were individually placed in metabolic cages (TSE phenoMaster/LabMaster, Germany) with free access to water and food and acclimatized for 24 h prior to monitoring respiratory parameters. All metabolic studies were conducted under the condition of temperature at 22 °C and a 12-h light/dark cycle. The following parameters of mice were recorded for continuous 24 h, including food and water intake, locomotor activity, gas exchange (O_2 and CO_2), and energy expenditure according to the manufacturer's guidelines (using PhenoMaster Software, TSE Systems). The respiratory exchange rate was estimated by calculating the ratio of VCO_2/VO_2 .

During the same week, rectal temperature was measured using a rectal probe equipped with a digital thermometer (Control Company, TX, USA) while the animals were awake without anesthesia.

2.6. Morphological analysis

Immunohistochemical staining was performed according to a standard protocol. Briefly, slides were dewaxed 3 times, each time for 15 min, then, slides were hydrated through an alcohol gradient, and soaked in PBS for 5 min. After blocking the non-specific binding site with 3% bovine serum albumin, slides were incubated with rabbit polyclonal anti-UCP1 primary antibody overnight at 4 °C, followed by incubation with an HRP-labeled secondary antibody. Digital images of all slides were taken using NanoZoomer 2.0-HT slide scanner (Hamamatsu, Japan).

2.7. Quantitative reverse Transcription-PCR (RT-qPCR)

Total RNA was extracted from adipose tissue using Trizol reagent (Invitrogen, CA, USA), and 1 µg of RNA was reverse transcribed into cDNA using a Takara kit (Takara, Japan). A 10 µL reaction mixture contained 5 µL of SYBR Green, 0.5 µL of each primer, 2 µL of template cDNA, and 2 µL of double-distilled water (ddH₂O). The reaction was run in an CFX96 real-time PCR detection system (Bio-Rad, CA, USA) following the manufacturer's instructions. All the expression levels of the target gene were normalized to β-actin, and the sequences of qPCR primers are shown in Table 1.

2.8. Western blotting

Adipose tissue was homogenized and lysed in ice-cold radio-immunoprecipitation assay (RIPA) buffer for 30 min. Lysates were centrifuged at 12,000 rpm for 20 min at 4 °C to collect the supernatants, then protein concentration was determined using a BCA assay. Western blot assay was carried out as previously reported (Xing et al., 2018). The relative density of bands was quantified and normalized to β-actin.

2.9. Fecal DNA extraction and amplification

Fecal samples were collected at the end of experiments, and frozen at -80 °C. Total bacterial DNA was isolated and measured for concentration using the NanoDrop instrument (Nano-Drop Technologies, Wilmington, DE). Universal primers (341F, 805R) were used to amplify the V3-V4 region of the 16S rDNA gene on a HiSeq sequencing platform (Illumina). The PCR products were purified and quantified with a Mini Elute PCR purification kit (AXYGEN, Hangzhou, China) and GeneAmp PCR System 9700 (Applied Biosystems, CA, USA), respectively. 16S rDNA gene sequencing was conducted on the Illumina HiSeq platform according to the standard protocol. Data were processed by FLASH V.1.2.7 software to obtain splicing sequences, namely primitive Tags data. Subsequently, the acquisition of high-quality Tags data from the Mosaic was performed using Trimmomatic V0.33 software. The conclusive valid data were obtained using UCHIME V4.2 software, following the confirmation and removal of chimeric sequences.

2.10. Fecal metabolites analysis

In the last week of diet intervention, fresh feces were collected and stored at -80 °C before analysis. The feces (50 mg) were extracted with 600 µL of methanol/water (2:1, v/v) solution and 20 µL of L-2-chlorophenylalanine (0.3 mg/mL) was used as internal standard. After homogenization and ultrasonic crushing, the samples were then centrifuged at 12,000×g for 10 min, and 200 µL supernatant was collected and dried in a vacuum concentrator. Then, all the samples were dissolved in 100 µL of methanol/water (1:1, v/v) solution for liquid chromatography-mass spectrometry (LC-MS) analysis.

Fecal metabolic profiling was analyzed using a UPLC-Q-Exactive-MS instrument (Thermo-Fisher) equipped with an Acquity UPLC BEH C18 (2.1 mm × 50 mm, 2.2 µm) chromatographic column and eluted with ultrapure water and acetonitrile both containing 0.1% formic acid (X. Li et al., 2022). The initial analysis of the raw data was carried out using Compound Discoverer software (v3.3.0). Principal component analysis (PCA) and orthogonal partial least squares discriminant analysis (OPLS-DA) were carried out to screen fecal metabolic profiling in

Table 1
Sequences of primers.

	Forward	Reverse
UCP1	TTCTGTGTAGCTACGGTGG	CCATCAAACCTGTTGAGCG
PGC-1α	ATGTGCAGCCAAGACTCTGTA	CGGTACACCACTTCAATCCAC
β-actin	GTGACGTTGACATCCGTAAGA	GCCGGACTCATCGTACTCC

different groups using SIMCA-P 16.0 (Sartorius Stedim Data Analytics AB, Umea, Sweden) software, and the variable importance projection (VIP) value was used to screen potential metabolic markers. In brief, VIP >1 and $p < 0.05$ were defined as differences based on the test of OPLS-DA. Moreover, the KEGG database was employed to screen the key metabolic pathways.

2.11. Statistical analysis

Data are presented as means ± SEM. ANOVA was used to compare sets of data. Tukey's test was used for the post hoc testing. All statistical analyses were carried out using GraphPad Prism. $P < 0.05$ was considered as significant. Correlation between gut microbial variation at the genus level and metabolic indicators was analyzed by Spearman's correlation analysis. Principal coordinate analysis (PCoA) plots were used to calculate the similarities and differences at OTU level among all groups.

3. Results

3.1. Naringin ameliorated obesity and consequent metabolic disorders in HFD-fed mice

To investigate the protective effect of naringin on obesity and related metabolic disorders, C57BL/6J mice were subjected to a high-fat diet (HFD) for 12 weeks. At the end of the dietary intervention, the body weight of HFD-fed mice was significantly increased compared to the low-fat diet (LFD)-fed group, indicating typical diet-induced obesity (DIO) (Fig. 1). Supporting this, HFD fed mice gained significant higher liver weight, eWAT weight, and fasting blood glucose than the LFD group which demonstrates that the administration of naringin effectively thwarted the diet-induced obesity (DIO) (Fig. 1A). Significantly, naringin treatment not only reduced liver and eWAT weight, but also decreased fasting blood glucose, compared with the HFD group (Fig. 1B-F). In line with this, naringin improved glucose tolerance in HFD-fed mice with a declined total area under the curve (AUC) in the OGTT test. Moreover, the levels of serum TG, TC, and LDL-C were reduced in HFD + naringin-fed mice (Fig. 1G-J). Thus, our results showed naringin prevented DIO of the mice, and ameliorated the metabolic profile resulted by HFD.

3.2. Naringin promoted energy expenditure

To test whether the obesity-protective effects of naringin are attributed to the promotion of thermogenic capacity, we conducted indirect calorimetry measurements using the Promethion metabolic cage system. Naringin-treated and control mice were individually housed in metabolic cages to enable the monitoring of gas exchange and energy expenditure. Consistent with a previous report, the high-fat diet (HFD) reduced energy expenditure and oxygen consumption (VO₂) compared to the low-fat diet (LFD) group, while the naringin intervention recovered this decrease significantly (Fig. 2A and B). However, we did not observe any alterations in the respiratory exchange ratio (RER) and locomotor activity (Fig. 2C and D). In line with the observed increase in energy expenditure and oxygen consumption, the dietary intervention of naringin resulted in a remarkable elevation in the mice's rectal temperature. Monitoring rectal temperature provides insights into the mice's ability to generate and regulate body heat, a crucial aspect of thermoregulation, as contrasted with the HFD control group (Fig. 2E). These data affirm that naringin induces thermogenesis in HFD-fed mice without altering locomotor activity.

3.3. Naringin elevated expression levels of genes and proteins involved in thermogenesis

To further investigate the mechanism of naringin-induced

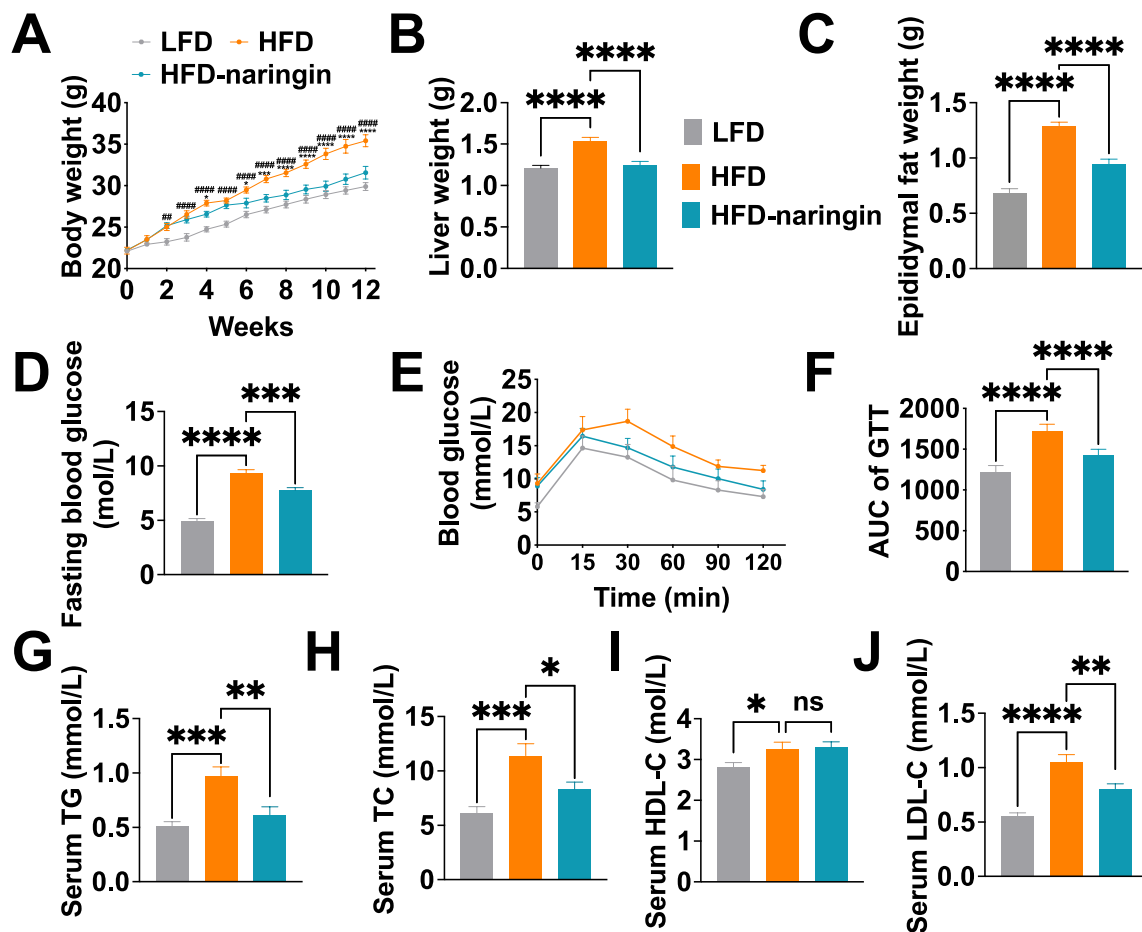


Fig. 1. Naringin attenuated high-fat diet-induced obesity and metabolic disorders. A. Body weight. B. Liver weight. C. Epididymal fat. D. Fasting glucose level. E and F. Glucose tolerance test (GTT) and area under the curve (AUC). G. Serum triglyceride. H. Serum total cholesterol. I. Serum high-density lipoprotein cholesterol. J. Serum low-density lipoprotein cholesterol. LFD, low-fat diet; HFD, high-fat diet plus solvent administration; HFD-naringin, high-fat diet plus naringin administration. * Indicates HFD group vs HFD-naringin group; # indicates HFD group vs LFD group. (A) ## $p < 0.01$, ### $p < 0.0001$, * $p < 0.05$, ** $p < 0.01$, *** $p < 0.001$, and **** $p < 0.0001$ in two-way ANOVA followed by post hoc Sidak tests. (D, F, G, H, I and J). * $p < 0.05$, ** $p < 0.01$, *** $p < 0.001$, and **** $p < 0.0001$ in one-way ANOVA followed by post hoc Tukey tests. Bars are mean \pm SEM (n = 10).

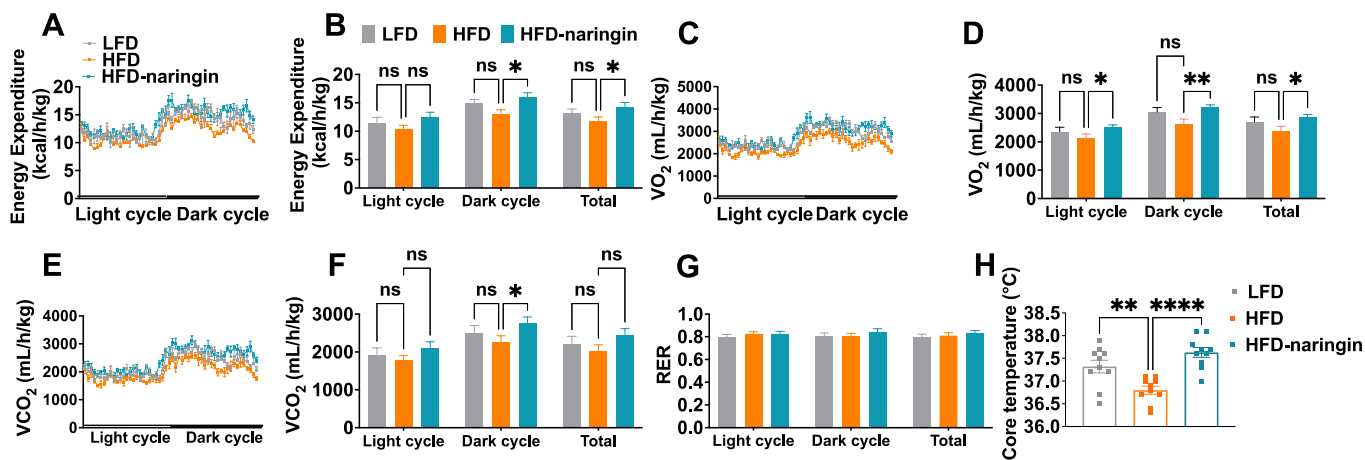


Fig. 2. Naringin promotes energy expenditure. A. Total energy expenditure and average energy expenditure in both the light and dark cycles. B. Total VO₂ consumption and average VO₂ consumption in both the light and dark cycles. C and D. Respiratory exchange ratio (RER) and ambulatory activity in both the light and dark cycles. E. Rectal temperature. LFD, low-fat diet; HFD, high-fat diet plus solvent administration; HFD-naringin, high-fat diet plus naringin administration. * Significantly different from high-fat diet group (HFD). * $p < 0.05$, ** $p < 0.01$, and **** $p < 0.0001$. in one-way ANOVA followed by post hoc Tukey tests. Bars are mean \pm SEM (n = 6).

thermogenesis, we collected iWAT and BAT of mice for the following RT-qPCR and Western blotting assay. We found that the mRNA and protein expression levels of thermogenic factors (UCP1 and PGC-1 α) was significantly upregulated after naringin treatment in both iWAT and BAT (Fig. 3B–D). Furthermore, our immunofluorescence results concurred with these observations, demonstrating heightened thermogenic activity in response to naringin, as evidenced by an enhanced expression of UCP1 protein within the BAT tissue (Fig. 3A).

3.4. Naringin altered gut microbiota composition

Gut microbiota showed comprehensive and essential roles in energy metabolism including lipogenesis, fat distribution, glucose homeostasis, and thermogenesis (Shelton et al., 2023). Furthermore, evidence reported the interaction between gut microbiota and such dietary functional compounds as curcumin stimulate thermogenesis and prevent DIO (Z. Han et al., 2021). To identify whether the gut microbiota participates in the anti-obesity actions of naringin, we further explored the effects of naringin dietary supplementation on the compositions of gut microbiota in HFD-fed mice using 16S rDNA sequencing. To investigate whether gut microbiota participate in the anti-obesity actions of naringin, we further explored the effects of naringin dietary supplementation on the compositions of gut microbiota in high-fat diet (HFD)-fed mice using 16S rDNA sequencing. To assess the alpha diversity of the gut microbiota, we calculated observed species, the Shannon index, the Simpson index, ACE, and the Chao1 index. As shown in Fig. 4, no significant changes were observed in the observed species and Shannon index between the HFD and HFD-naringin groups (Fig. 4A and B). However, naringin significantly increased the Simpson, ACE, and Chao1

indices (Fig. 4C–E), indicating that naringin enhanced the diversity of gut microbiota in obese mice. Principal Coordinates Analysis (PCoA) revealed separation among the low-fat diet (LFD), HFD, and HFD-naringin individuals based on the first two principal components (PC) scores, which accounted for 34.68% and 23.44% of the total variations (Fig. 4F). This result indicates that naringin had a significant influence on the overall composition of the mice's gut microbial communities.

Taxonomy-based comparisons of the gut microbiota were performed to compare the overall community compositions of gut microbiota from the mice fed with different diets. The phylum analysis revealed that *Firmicutes* was the most predominant phylum, contributing relative abundances of 58.99, 78.06 and 53.56% to the gut microbiota composition of the LFD, HFD, and HFD-naringin mice, respectively, followed by *Bacteroidota* (9.22, 2.98 and 16.92%) (Fig. 5A). In addition, Linear Discriminant Analysis Effect Size (LEfSe) analysis was performed to identify the characteristic bacteria of the LFD, HFD, and HFD-naringin groups. A total of 29 operational taxonomic units (OUTs) were notably different among these three groups. Notably, in the HFD-naringin group, there were 16 OUTs prominent different from other groups, including *Bacteroidales*, *Bacteroidia*, *Bacteroidota*, and *Oscillospirales*, etc. (Fig. 5B). At the genus level, naringin treatment significantly triggered differences in species abundance, and the relative abundance of genus *Bifidobacterium* and *Lachnospiraceae_bacterium_28-4* were remarkably higher in the HFD-naringin group than the HFD group. The abundance of *Lachnospiraceae_bacterium_DW59* and *Dubosiella_newyorkensis* were significantly reduced in naringin-treated mice (Fig. 5C–E).

For assurance that the modification of gut microbiota by naringin

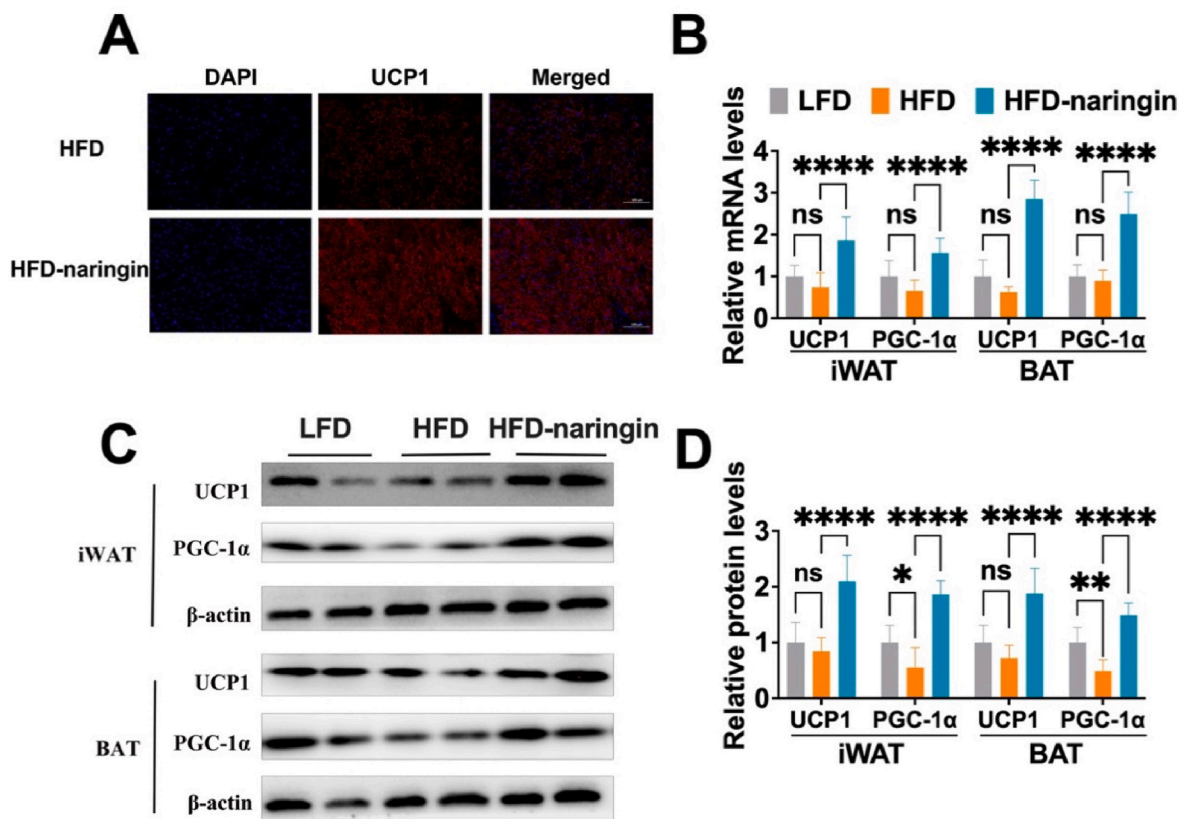


Fig. 3. Naringin promoted expression levels of thermogenic related protein (A, C and D) and mRNA (B) in the brown adipose tissue (BAT) and the inguinal white adipose tissue (iWAT). A. Immunofluorescent staining for UCP1 (red) in BAT from HFD and HFD-naringin treated mice. Nuclei are stained with DAPI (blue). B. mRNA expression levels of thermogenic genes in iWAT and BAT. C and D. Protein expression levels related to thermogenesis in iWAT and BAT. LFD, low-fat diet; HFD, high-fat diet plus solvent administration; HFD-naringin, high-fat diet plus naringin administration. * $p < 0.05$, ** $p < 0.01$, *** $p < 0.001$, **** $p < 0.0001$. Bars are mean \pm SEM ($n = 6$). (For interpretation of the references to colour in this figure legend, the reader is referred to the Web version of this article.)

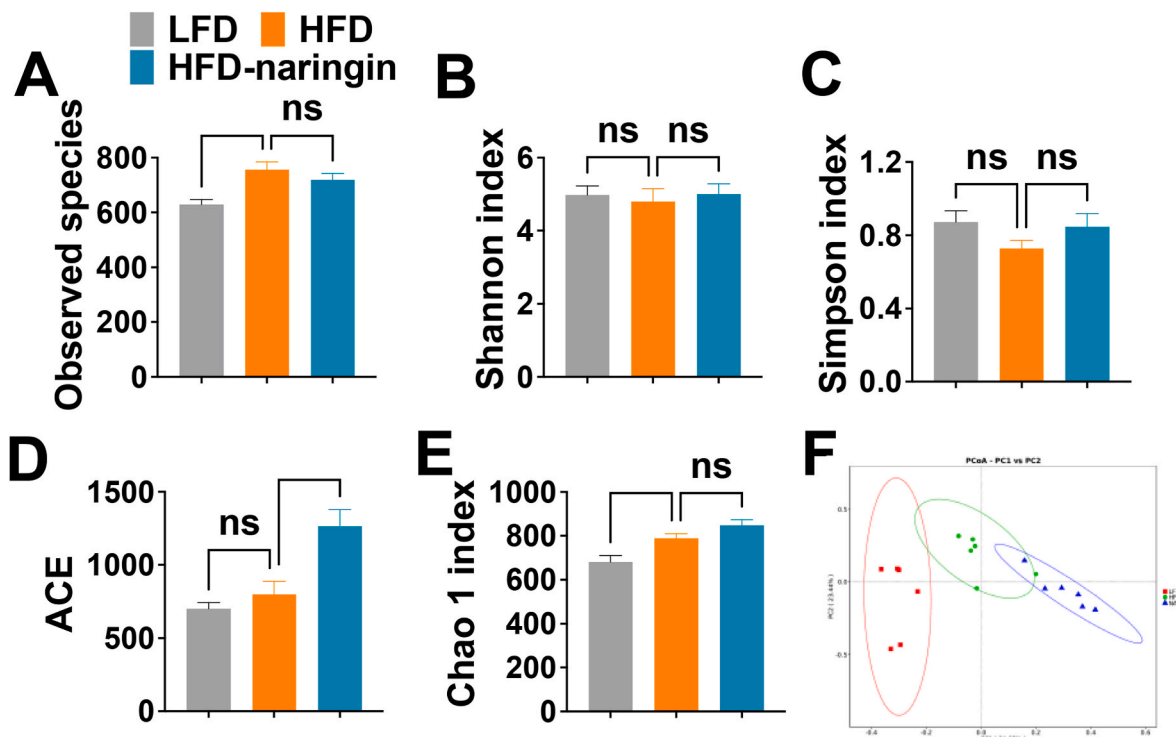


Fig. 4. Naringin supplementation altered the gut microbiota compositions in HFD-fed mice. A. Observed species. B. Shannon index. C. Simpson index. D. ACE index. E. Chao 1 index. F. Principal coordinate analysis (PCoA) of gut microbiota between all groups. LFD, low-fat diet; HFD, high-fat diet plus solvent administration; HFD-naringin, high-fat diet plus naringin administration. * $p < 0.05$, ** $p < 0.01$, and **** $p < 0.0001$. in one-way ANOVA followed by post hoc Tukey tests. Bars are mean \pm SEM (n = 6). Bars are mean \pm SEM (n = 6).

correlated with the metabolic parameters of mice, we constructed a correlation map in our study by analyzing various adiposity-related parameters and specific bacterial taxa. As depicted in Fig. 5F, the genus *Bifidobacterium*, notably increased by naringin administration, exhibited a positive correlation with the expression levels of thermogenic genes and a negative correlation with body weight and epididymal white adipose tissue (eWAT) weight. Collectively, these results indicate that the naringin-induced modification of gut microbiota could influence the body weight and thermogenic genes of high-fat diet (HFD)-induced obese mice.

3.5. Untargeted analysis of fecal metabolites

In this study, the fecal metabolic profiles were mapped using untargeted metabolomics techniques with both positive and negative models. As shown in Fig. 6A and B, the principal component analysis (PCA) and Orthogonal partial least squares discrimination analysis (OPLS-DA) results showed distinguishable fecal metabolites between HFD-fed mice and HFD + naringin-fed mice. Based on the results of the permutation test, we ensure that all OPLS-DA models were reliable without overfitting (Fig. 6C). Moreover, the volcano plot displayed remarkable changes in fecal metabolites in mice after naringin treatment (Fig. 6D), and overall, 298 metabolites were upregulated and 223 metabolites were downregulated by naringin administration, respectively.

Differential fecal metabolites between the HFD-fed mice and HFD + naringin-fed mice were screened out under the standard of $VIP > 1$ and $p < 0.05$. As shown in Fig. 7, the top 50 metabolites were clustered in the heatmap, and the results showed that the contents of beneficial substances such as tyrosol, taurine, thymol, and Vitamin C in the process of alleviating obesity and metabolic disorders were significantly increased after naringin intervention. Interestingly and importantly, according to the screened differential metabolites, further KEGG enrichment analysis

was conducted. These potential biomarkers were enriched in multiple metabolic pathways, including alanine, aspartate, and glutamate metabolism, citrate cycle, and biosynthesis of unsaturated fatty acids (Fig. 8).

3.6. Gut microbiota mediate the weight-control effect of naringin

For further clarification of the causative role of the gut microbiota in mediating the anti-obesity effects of naringin, we exposed HFD-fed mice to an antibiotics cocktail via drinking water to reduce the majority of gut microbiota. As expected, the effects of naringin on weight control were abrogated after antibiotics intervention (Fig. 9A). Notably, the naringin-treated microbiota-reduced (HFD-naringin-Abs) mice still maintained a relatively lower final body weight without statistical significance after a 10-week intervention of antibiotics. Furthermore, there were no alterations observed in liver weight, eWAT weight, and glucose tolerance among the mice treated with antibiotics regardless of whether they were introduced to naringin or not, under the HFD condition (Fig. 9B and C). Additionally, the increase in energy expenditure and overexpression of UCP1 and PGC-1 α in BAT and iWAT were abolished after antibiotics intervention (Fig. 9D and E). These results suggested that the reduction of gut microbes could effectively control weight and blood glucose and eliminate overexpression of thermogenic genes in HFD + naringin-fed mice, which indicated that the intestine might be the primary target tissue for naringin to enhance thermogenesis and ameliorate obesity and related symptoms.

4. Discussion

Obesity has become a major public health burden worldwide. Along with traditional therapeutic methods for obesity, such as increasing physical activity to elevate energy expenditure or restricting energy intake, a promising strategy for combating obesity is increasing non-

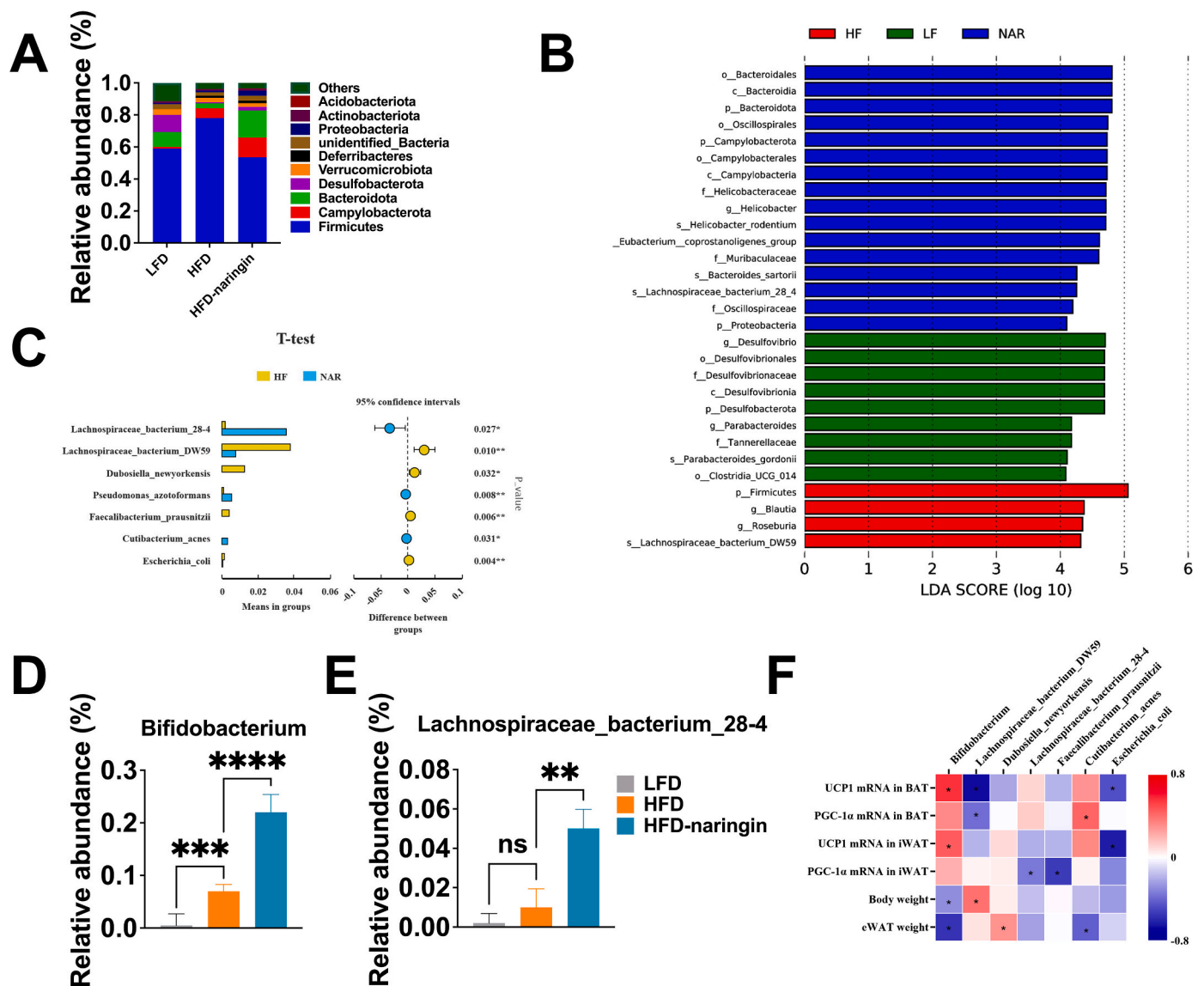


Fig. 5. Naringin changed the gut microbiota composition. A. The relative abundance of the top ten abundant bacteria at the phylum level. B. Linear Discriminant Analysis Effect Size (LEfSe) analysis of the characteristic genera of gut microbiota. C. T-test analysis of differences of the gut bacteria at the genus level between the HFD group and the HFD-naringin group. D and E. The relative abundance of *Bifidobacterium* and *Lachnospiraceae_bacterium_28-4* at the genus level. F. Heatmap of the Spearman's correlations between the bacterial genera and the metabolic parameters in mice treated with HFD alone or HFD plus naringin. LFD, low-fat diet; HFD-V, high-fat diet plus solvent administration; HFD-naringin, high-fat diet plus naringin administration. * $p < 0.05$, ** $p < 0.01$, and *** $p < 0.0001$. In one-way ANOVA followed by post hoc Tukey tests. Bars are mean \pm SEM ($n = 6$).

shivering thermogenesis (Z. Han et al., 2021; Thyagarajan and Foster, 2017). Naringin, a prominent bioactive flavanone from citrus fruit, has been reported to show antihyperglycemic and antioxidant properties (Raja Kumar et al., 2019). However, whether naringin affects non-shivering thermogenesis and the corresponding underlying mechanisms remain unclarified. In this study, we investigated the effect of naringin on body weight gain of the diet-induced obesity (DIO) mice model. Our study found that daily administration of naringin (100 mg/kg/day, gavage) for 12 weeks significantly mitigated the increase in body weight, and concurrently reduced liver, and eWAT weight compared with HFD treated mice. In line with this, the naringin treated mice showed lower plasma TG, TC, LDL-C, and fasting glucose levels and improved glucose tolerance. Notably, our data also showed naringin promoted non-shivering thermogenesis, and this effect appears to be primarily localized within BAT (Cohen and Spiegelman, 2015; Ma et al., 2015). UCP1 is one of the most representative thermogenic effectors and controlling weight gain, and the complex of PGC-1 α with peroxisome

proliferator-activated receptor γ (PPAR γ) regulates the expression of UCP1 and manipulating thermogenesis (Chouchani and Kajimura, 2019; Handschin and Spiegelman, 2006; Nierenberg et al., 2018). Intriguingly, our data showed HFD-fed mice administrated with naringin increased energy expenditure and oxygen consumption accompanied by the upregulated UCP1 in BAT. In support of this, we also found a robust augmentation in both mRNA and protein expression levels of UCP1 and PGC-1 α in BAT induced by the dietary naringin treatment. Our finding also be supported by previous *in vitro* data, which showed a 3T3-L1 adipocyte was treated with naringin (6.25–25 μ M) for 48 h and increasing UCP1 and PGC-1 α gene expression. WAT is incredibly dynamic and responds to various stimuli, including environmental temperature and phytochemicals, such as curcumin and fucoxanthin (X. Li et al., 2022). Additionally, the process of “browning” WAT has received increased attention due its potential application in fighting with obesity (Vitali et al., 2012). Our data showed the naringin treatment significantly increased the expression of such biomarkers in the process of

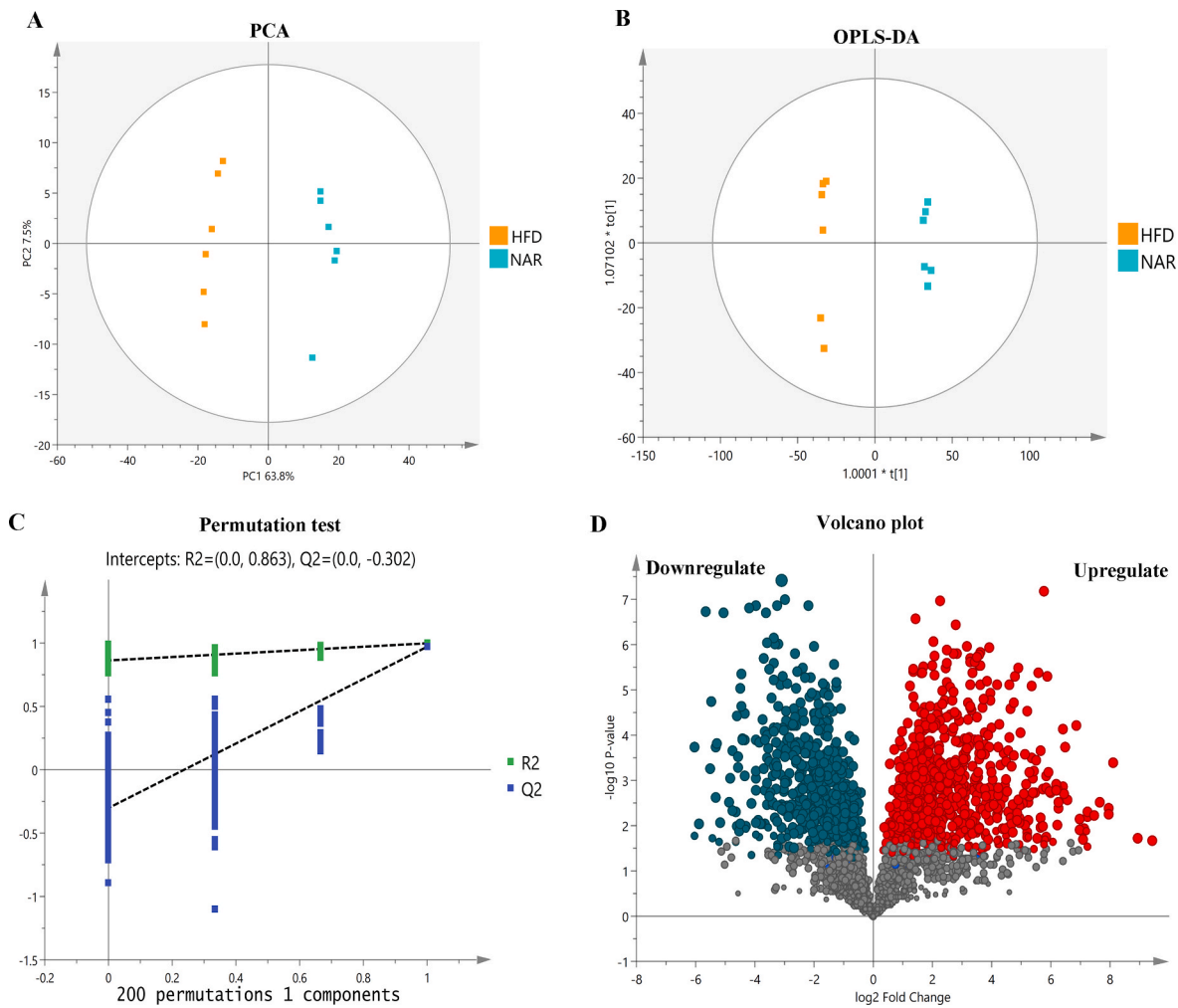


Fig. 6. Naringin affects the fecal metabolites in HFD-fed mice. A. Principal component analysis (PCA) plot. B. Orthogonal partial least squares discrimination analysis (OPLS-DA) plot. C. Permutation test plot based on OPLS-DA methods. D. Volcano plot based on the altered metabolites of the HFD-naringin group compared with the HFD group; n = 6.

“browning” of iWAT as UCP1 and PGC-1 α (Fm et al., 2012; X et al., 2016). Collectively, our findings suggested naringin stimulates BAT thermogenesis and promotes iWAT browning via a PGC-1 α /UCP1 mechanism.

It has been postulated that gut microbiota plays multiple roles in regulating energy homeostasis. Gut microbiota could change the bioavailability of dietary functional components, affecting the energy intake of the host, and alterations in gut microbiota population can influence BAT thermogenesis and whole-body energy expenditure (Chevalier et al., 2015; M et al., 2014; Turnbaugh et al., 2006; Yuan et al., 2019). Cumulative evidence showed a variety of phytochemicals, such as citrus polymethoxyflavones, cordycepin and vanillin can reduce body weight accompanied by alterations in the population of gut microbiota (An et al., 2018; Shi et al., 2019; Zeng et al., 2020). Indeed, the treatment with such phytochemicals promoted lipolysis and thermogenesis. However, there is a need for more direct evidence to establish a clear link between the reshaping in gut microbiota and metabolic effects of such phytochemicals. In the present study, we also found that naringin treatment could modify gut microbiota population. And specifically, the Alpha diversity index indicated that naringin treatment increased the species diversity of gut microbiota. The following PCoA analysis revealed separation among the LFD, HFD, and HFD-naringin mice. Subsequently, we analyzed the specific changes in the gut microbiota at the phylum and genus levels with the main phyla observed in the present study including *Firmicute*, *Campylobacterota*, *Bacteroidetes*.

At the genus level, naringin treatment significantly triggered differences in species abundance, our data showed that naringin treatment significantly increased the abundance of *Bifidobacterium* and *Lachnospiraceae_bacterium_28_4*. These findings align with previous research wherein naringin’s effect on gut microbiota and HFD significantly increased the abundance of *Firmicutes*. (Sang et al., 2021; Turnbaugh et al., 2006). Spearman’s correlation analysis also showed that the abundance of *Bifidobacterium* was positively correlated to expression levels of thermogenic genes and negatively correlated with body weight and eWAT weight, which suggested a potential link between the abundance of *Bifidobacterium* and the metabolic effect of naringin and combating obesity. This result also confirmed the study by Turnbaugh, P.J. et al., that naringin treatment notably increased the abundance of *Bacteroidetes*, which was positively correlated to weight loss (Turnbaugh et al., 2006). Previous studies indicated that *Bifidobacterium* could activate G protein-coupled receptor 5 (TGR-5), as a metabolic regulator, thereby regulating metabolism and combating obesity (M. Li et al., 2022; Zhao et al., 2023). Furthermore, *Lachnospiraceae_bacterium_28_4* was also indicated to be negatively related to obesity and serum lipid parameters (Hernández et al., 2019). *Dubosiella_newyorkensis* has been noted to exhibit anti-aging properties comparable to those of resveratrol. However, its presence significantly escalated in a mouse model with hyperhomocysteinemia and glucose intolerance induced by a high-methionine diet (W. Li et al., 2023; T.-H. Liu et al., 2023). In this study, the relative abundance of *Dubosiella_newyorkensis* was

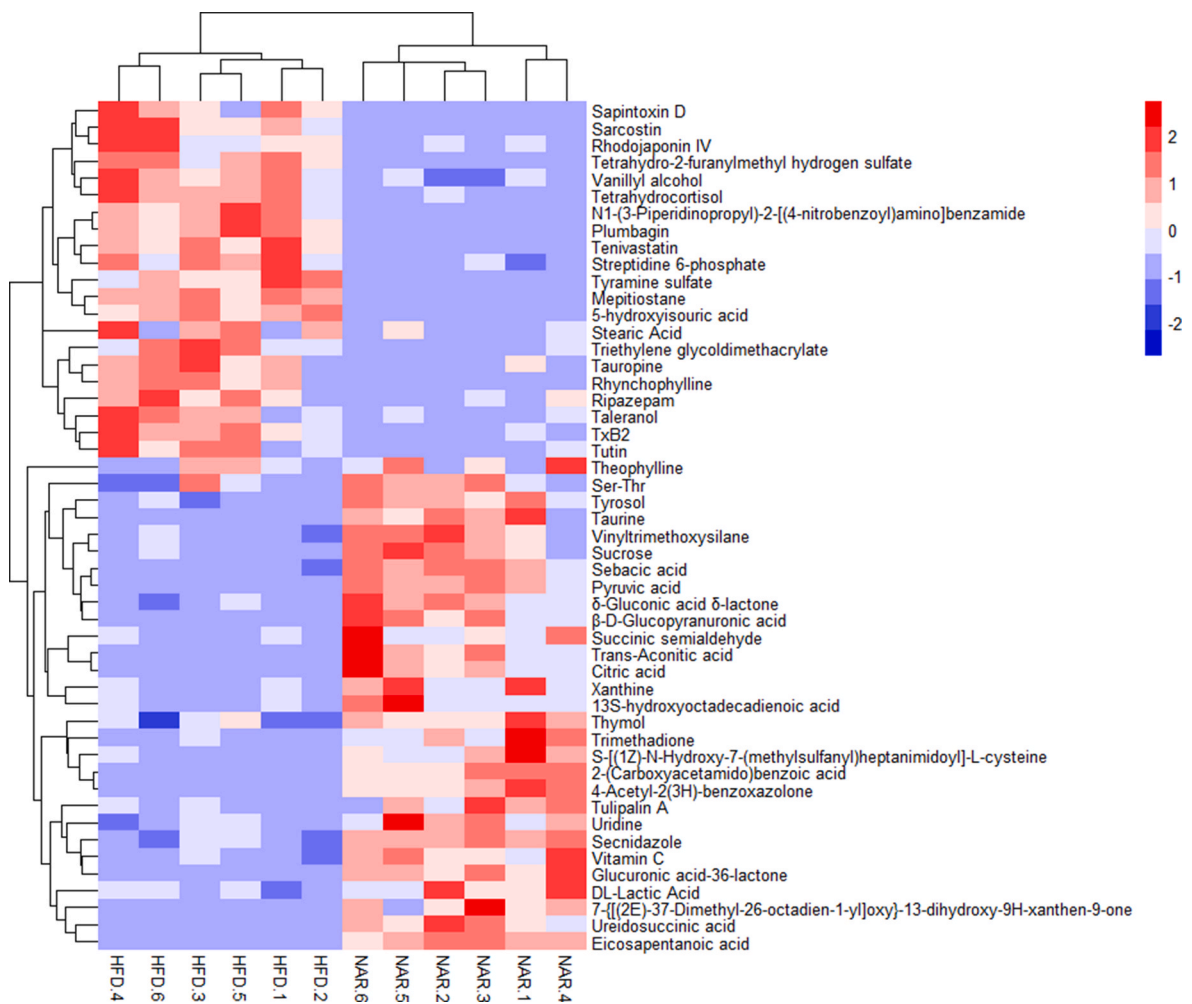


Fig. 7. Heatmap of the top 50 different metabolites in the HFD and HFD-naringin groups.

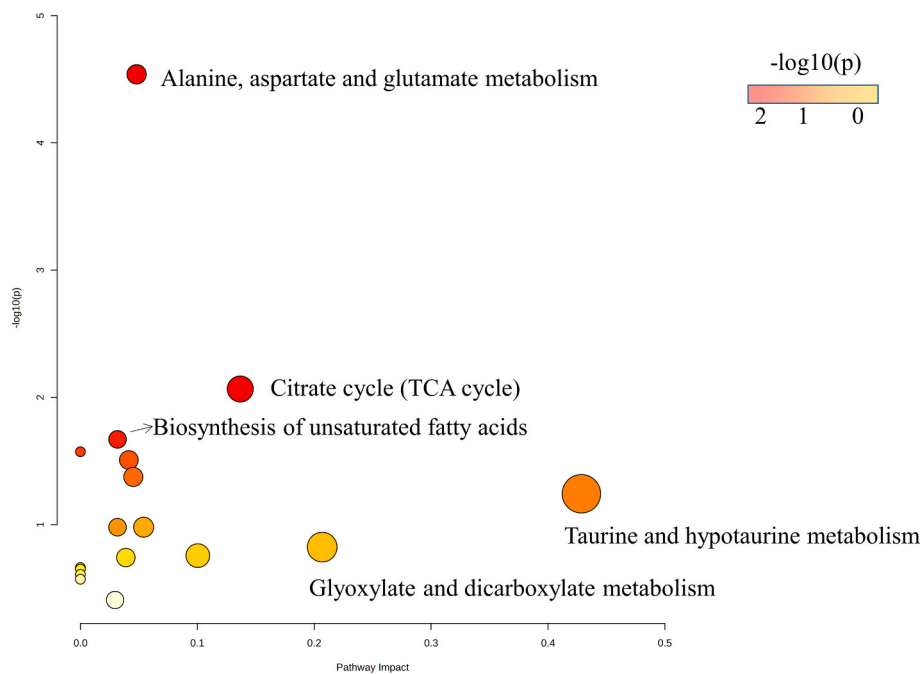


Fig. 8. Naringin regulates the metabolic pathways in HFD-fed mice.

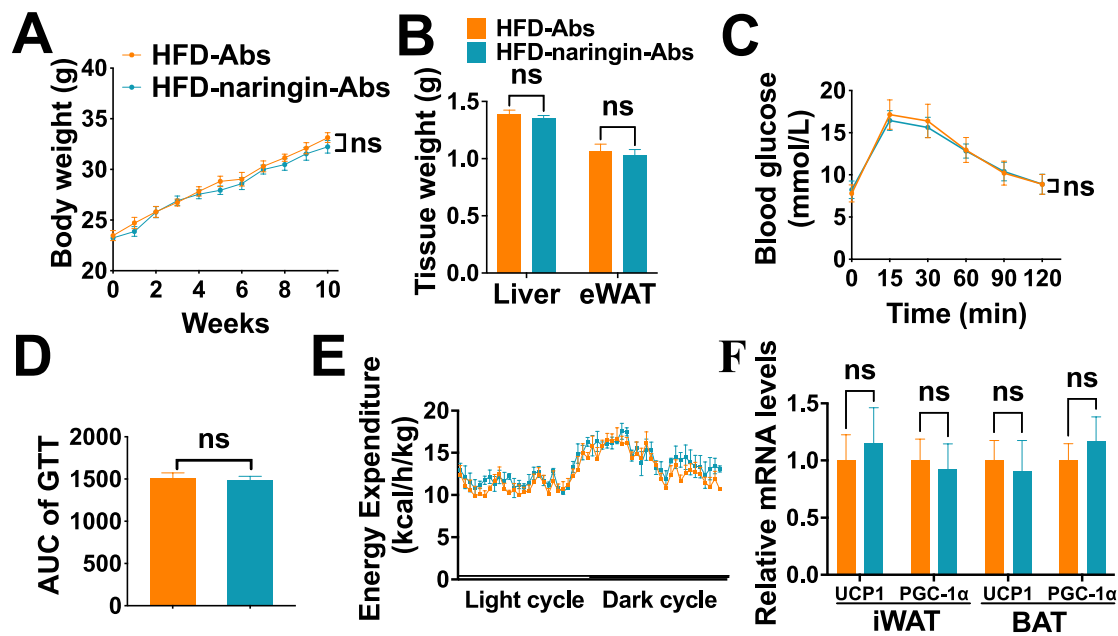


Fig. 9. Gut microbiota mediates the therapeutic effects of naringin treatment. The mice were fed an HFD together with an antibiotics cocktail in drinking water and gavage with vehicle or naringin (100 mg/kg/d) for 10 weeks ($n = 10$). A. Body weight of antibiotics-treated mice. B. Tissue weight. C and D. Glucose tolerance test (GTT) and area under the curve (AUC). E. Total energy expenditure of mice (after 10 weeks of feeding) over a 24-h period ($n = 5$). F. mRNA expression levels of genes related to thermogenesis in iWAT and BAT. Data are shown as mean \pm SEM.

significantly reduced after naringin administration, so more studies are needed to verify the exactly physiological effect of this bacteria.

These findings suggest that changes in the gut microbiota might be associated with weight control effect of naringin in the DIO mice. However, further investigation is required to identify whether the naringin-induced upregulation of such thermogenic genes is directly positively linked with the naringin-induced increased population of *Bifidobacterium*. The fecal metabolic profiles were mapped in our study, and the results showed distinguishable differences in fecal metabolites between HFD-fed mice and HFD + naringin-fed mice. Compared with HFD group, the naringin treatment significantly increased the production of tyrosol, taurine, thymol, and vitamin C, and notably, these compounds have been showed positive effects on thermogenesis and browning of WAT (Basch et al., 2004; Choi et al., 2017; B. Lee et al., 2022; X. Li et al., 2022). Previously, we reported that tyrosol may interact with PPAR γ as an agonist, stimulating thermogenesis of WAT, while taurine has been showed acted as a thermoregulator via central nervous system. Interestingly, the interplay between bacterial metabolites and PPAR γ has been reported to modulate multiple aspect of energy metabolism. Recently, phenyllactic acid, a *Lactobacillus*-derived metabolite, was shown to interact with PPAR γ , regulating intestinal lipid metabolism and preventing HFD-induced metabolic dysfunction (GBD 2015 Obesity Collaborators et al., 2017). These findings suggested bacterial metabolites may play important roles in the protective effects of naringin via various mechanisms, while the individual mediating roles of such bacterial metabolites as tyrosol, taurine, thymol, and vitamin C still need to be further clarified.

Previous research reported that microbiota depletion impairs the thermogenesis of BAT and browning of WAT (Cani et al., 2019; B. Li et al., 2019), this led us to further test if gut microbiota is required for naringin to regulate energy metabolism. Our present study showed that microbiota depletion abolished the naringin-induced amelioration in metabolic outcomes of DIO mice, such as whole-body weight, liver, and eWAT weight, as well as glucose tolerance. Subsequently, the effects of naringin on energy expenditure, oxygen consumption, and the expression thermogenic genes in both BAT and iWAT were also attuned in the

antibiotics-induced microbiota depletion mice model. These results indicated that gut microbiota is necessary in the regulation of naringin in energy metabolism. In line with our finding, curcumin has been shown that enhance thermogenesis, which requires the presence of gut microbiota (Cheng et al., 2022). Overall, our findings underscore the significance of the interplay between naringin and gut bacteria in the regulation of naringin in energy metabolism. Additionally, they unveil a varied array of effects resulting from this interaction through distinct underlying mechanisms.

Although the obesity rate in females is much higher than in males, obesity studies in rodents are mainly conducted in males due to concerns that the estrus cycle of females may make female models inherently more variable than male models (Garawi et al., 2014; NCD Risk Factor Collaboration (NCD-RisC), 2016). Sexual specific metabolic profiles for treatment have been reported in animal models, therefore, the effect of naringin observed in this study should be confirmed in female obese mice (Mauvais-Jarvis et al., 2017). The lack of positive controls such as β 3-adrenergic receptor (CL-316,243) and PPAR α agonists (fenofibrate), with known activity to stimulate UCP1 expression and induce thermogenesis is another limitation (Burl et al., 2018). Thus, future investigations are warranted to elucidate the precise molecular pathways involved.

5. Conclusion

The present study indicates that naringin prevented diet-induced obesity (DIO) and comprehensively ameliorates the consequent metabolic dysfunctions. Importantly, the dietary naringin supplement promotes brown adipose tissue (BAT) thermogenesis and stimulates browning of inguinal white adipose tissue (iWAT) via the PGC-1 α /PPAR γ mechanism. Furthermore, naringin alters the composition of the gut microbiota, and simultaneously modifies gut bacterial metabolites. This may act as a pivotal factor contributing to the weight-control effect of naringin. Given the abundance of naringin in citrus fruit, our findings provide solid evidence for the weight-control effects of citrus fruit consumption.

CRedit authorship contribution statement

Xiaoping Li: contributed to, Investigation, and, Validation, of the study. **Zhao Yao:** contributed to, Methodology. **Xinyue Qi:** contributed to conduct of the study and data interpretation. **JinLing Cui:** contributed to, Methodology. **Yuliang Zhou:** contributed to conduct of the study and data interpretation. **Yihong Tan:** contributed to conduct of the study and data interpretation. **Xiaojun Huang:** contributed to the manuscript writing. **Hui Ye:** contributed to the study design, data interpretation, and manuscript writing.

Declaration of competing interest

The authors declare that they have no known competing financial interests or personal relationships that could have appeared to influence the work reported in this paper.

Data availability

Data will be made available on request.

Acknowledgments

This work was supported by grants from National Research Foundation Singapore under its Young Individual Research Grant (023567-00001) to HY and administered by Singapore Ministry of Health's National Medical Research Council, Singapore MOE AcRF Tier 1 (RG90/23) to HY, NTU-Research Scholarship (R2301921) to XQ, Nature Science Foundation of Jiang Xi (General Program, 20224BAB205040) to XJ. We also would like to thank Dr. Phillip Grant for his great help on the proofreading.

References

- Alam, Md A., Kauter, K., Brown, L., 2013. Naringin improves diet-induced cardiovascular dysfunction and obesity in high carbohydrate, high fat diet-fed rats. *Nutrients* 5 (3), 637–650. <https://doi.org/10.3390/nu5030637>.
- An, Y., Li, Y., Wang, X., Chen, Z., Xu, H., Wu, L., Li, S., Wang, C., Luan, W., Wang, X., Liu, M., Tang, X., Yu, L., 2018. Cordycepin reduces weight through regulating gut microbiota in high-fat diet-induced obese rats. *Lipids Health Dis.* 17 (1), 276. <https://doi.org/10.1186/s12944-018-0910-6>.
- Anhê, F.F., Roy, D., Pilon, G., Dudonné, S., Matamoros, S., Varin, T.V., Garofalo, C., Moine, Q., Desjardins, Y., Levy, E., Marette, A., 2015. A polyphenol-rich cranberry extract protects from diet-induced obesity, insulin resistance and intestinal inflammation in association with increased Akkermansia spp. Population in the gut microbiota of mice. *Gut* 64 (6), 872–883. <https://doi.org/10.1136/gutjnl-2014-307142>.
- Basch, E., Ulbricht, C., Hammerness, P., Bevins, A., Sollars, D., 2004. Thyme (*Thymus vulgaris* L.), *thymol*. *J. Herb. Pharmacother.* 4 (1), 49–67.
- Burl, R.B., Ramseyer, V.D., Rondini, E.A., Pique-Regi, R., Lee, Y.-H., Granneman, J.G., 2018. Deconstructing adipogenesis induced by β -adrenergic receptor activation with single-cell expression profiling. *Cell Metabol.* 28 (2), 300–309.e4. <https://doi.org/10.1016/j.cmet.2018.05.025>.
- Cani, P.D., Van Hul, M., Lefort, C., Depommier, C., Rastelli, M., Everard, A., 2019. Microbial regulation of organismal energy homeostasis. *Nat. Metab.* 1 (1) <https://doi.org/10.1038/s42255-018-0017-4>. Article 1.
- Chen, R., Qi, Q.-L., Wang, M.-T., Li, Q.-Y., 2016. Therapeutic potential of naringin: an overview. *Pharmaceut. Biol.* 54 (12), 3203–3210. <https://doi.org/10.1080/13882009.2016.1216131>.
- Cheng, L., Shi, L., He, C., Wang, C., Lv, Y., Li, H., An, Y., Dai, H., Duan, Y., Zhang, H., Huang, Y., Fu, W., Meng, Y., Zhao, B., 2022. Rutin-activated adipose tissue thermogenesis is correlated with increased intestinal short-chain fatty acid levels. *Phytother. Res.* PTR 36 (6), 2495–2510. <https://doi.org/10.1002/ptr.7462>.
- Chevalier, C., Stojanović, O., Colin, D.J., Suarez-Zamorano, N., Tarallo, V., Veyrat-Durebex, C., Rigo, D., Fabbiano, S., Stevanović, A., Hagemann, S., Montet, X., Seimbille, Y., Zamboni, N., Hapfelmeyer, S., Trajkovski, M., 2015. Gut microbiota orchestrates energy homeostasis during cold. *Cell* 163 (6), 1360–1374. <https://doi.org/10.1016/j.cell.2015.11.004>.
- Choi, J.H., Kim, S.W., Yu, R., Yun, J.W., 2017. Monoterpene phenolic compound thymol promotes browning of 3T3-L1 adipocytes. *Eur. J. Nutr.* 56 (7), 2329–2341. <https://doi.org/10.1007/s00394-016-1273-2>.
- Chouchani, E.T., Kajimura, S., 2019. Metabolic adaptation and maladaptation in adipose tissue. *Nat. Metab.* 1 (2), 189–200. <https://doi.org/10.1038/s42255-018-0021-8>.
- Cohen, P., Kajimura, S., 2021. The cellular and functional complexity of thermogenic fat. *Nat. Rev. Mol. Cell Biol.* 22 (6), 393–409. <https://doi.org/10.1038/s41580-021-00350-0>.

- Cohen, P., Spiegelman, B.M., 2015. Brown and beige fat: molecular parts of a thermogenic machine. *Diabetes* 64 (7), 2346–2351. <https://doi.org/10.2337/db15-0318>.
- Fernández-Verdejo, R., Marlatt, K.L., Ravussin, E., Galgani, J.E., 2019. Contribution of brown adipose tissue to human energy metabolism. *Mol. Aspect. Med.* 68, 82–89. <https://doi.org/10.1016/j.mam.2019.07.003>.
- Fm, F., S, K., N, D., Ec, F., Rj, M., F, V., J, W., A, K., Js, F., E, M.-F., Bm, S., 2012. FGF21 regulates PGC-1 α and browning of white adipose tissues in adaptive thermogenesis. *Gene Dev.* 26 (3) <https://doi.org/10.1101/gad.177857.111>.
- Garawi, F., Devries, K., Thorogood, N., Uauy, R., 2014. Global differences between women and men in the prevalence of obesity: is there an association with gender inequality? *Eur. J. Clin. Nutr.* 68 (10), 1101–1106. <https://doi.org/10.1038/ejcn.2014.86>.
- GBD 2015 Obesity Collaborators, Afshin, A., Forouzanfar, M.H., Reitsma, M.B., Sur, P., Estep, K., Lee, A., Marczak, L., Mokdad, A.H., Moradi-Lakeh, M., Naghavi, M., Salama, J.S., Vos, T., Abate, K.H., Abbafati, C., Ahmed, M.B., Al-Aly, Z., Alkerwi, A., Al-Raddadi, R., et al., 2017. Health effects of overweight and obesity in 195 countries over 25 years. *N. Engl. J. Med.* 377 (1), 13–27. <https://doi.org/10.1056/NEJMoa1614362>.
- Guo, B., Liu, B., Wei, H., Cheng, K.-W., Chen, F., 2019. Extract of the microalga *Nitzschia laevis* prevents high-fat-diet-induced obesity in mice by modulating the composition of gut microbiota. *Mol. Nutr. Food Res.* 63 (3), e1800808 <https://doi.org/10.1002/mnfr.201800808>.
- Han, Y., Su, J., Liu, X., Zhao, Y., Wang, C., Li, X., 2017. Naringin alleviates early brain injury after experimental subarachnoid hemorrhage by reducing oxidative stress and inhibiting apoptosis. *Brain Res. Bull.* 133, 42–50. <https://doi.org/10.1016/j.brainresbull.2016.12.008>.
- Han, Z., Yao, L., Zhong, Y., Xiao, Y., Gao, J., Zheng, Z., Fan, S., Zhang, Z., Gong, S., Chang, S., Cui, X., Cai, J., 2021. Gut microbiota mediates the effects of curcumin on enhancing Ucp1-dependent thermogenesis and improving high-fat diet-induced obesity. *Food Funct.* 12 (14), 6558–6575. <https://doi.org/10.1039/d1fo00671a>.
- Handschin, C., Spiegelman, B.M., 2006. Peroxisome proliferator-activated receptor gamma coactivator 1 coactivators, energy homeostasis, and metabolism. *Endocr. Rev.* 27 (7), 728–735. <https://doi.org/10.1210/er.2006-0037>.
- Hernández, M.A.G., Canfora, E.E., Jocken, J.W.E., Blaak, E.E., 2019. The short-chain fatty acid acetate in body weight control and insulin sensitivity. *Nutrients* 11 (8), 1943. <https://doi.org/10.3390/nu11081943>.
- Kumar, P., Kumar, A., 2010. Protective effect of hesperidin and naringin against 3-nitropropionic acid induced Huntington's like symptoms in rats: possible role of nitric oxide. *Behav. Brain Res.* 206 (1), 38–46. <https://doi.org/10.1016/j.bbr.2009.08.028>.
- Kurylowicz, A., Puzianowska-Kuźnicka, M., 2020. Induction of adipose tissue browning as a strategy to combat obesity. *Int. J. Mol. Sci.* 21 (17), 6241. <https://doi.org/10.3390/ijms21176241>.
- Lee, B., An, H.J., Kim, D.H., Lee, M.-K., Jeong, H.H., Chung, K.W., Go, Y., Seo, A.Y., Kim, I.Y., Seong, J.K., Yu, B.P., Lee, J., Im, E., Lee, I.-K., Lee, M.-S., Yamada, K., Chung, H.Y., 2022. SMP30-mediated synthesis of vitamin C activates the liver PPAR α /FGF21 axis to regulate thermogenesis in mice. *Exp. Mol. Med.* 54 (11) <https://doi.org/10.1038/s12276-022-00888-9>. Article 11.
- Li, B., Li, L., Li, M., Lam, S.M., Wang, G., Wu, Y., Zhang, H., Niu, C., Zhang, X., Liu, X., Hambly, C., Jin, W., Shui, G., Speakman, J.R., 2019. Microbiota depletion impairs thermogenesis of Brown adipose tissue and browning of white adipose tissue. *Cell Rep.* 26 (10), 2720–2737.e5. <https://doi.org/10.1016/j.celrep.2019.02.015>.
- Li, G., Xie, C., Lu, S., Nichols, R.G., Tian, Y., Li, L., Patel, D., Ma, Y., Brocker, C.N., Yan, T., Krausz, K.W., Xiang, R., Gavrilova, O., Patterson, A.D., Gonzalez, F.J., 2017. Intermittent fasting promotes white adipose browning and decreases obesity by shaping the gut microbiota. *Cell Metabol.* 26 (4), 672–685.e4. <https://doi.org/10.1016/j.cmet.2017.08.019>.
- Li, M., Wang, S., Li, Y., Zhao, M., Kuang, J., Liang, D., Wang, J., Wei, M., Rajani, C., Ma, X., Tang, Y., Ren, Z., Chen, T., Zhao, A., Hu, C., Shen, C., Jia, W., Liu, P., Zheng, X., Jia, W., 2022. Gut microbiota-bile acid crosstalk contributes to the rebound weight gain after calorie restriction in mice. *Nat. Commun.* 13 (1) <https://doi.org/10.1038/s41467-022-29589-7>. Article 1.
- Li, W., Jia, Y., Gong, Z., Dong, Z., Yu, F., Fu, Y., Jiang, C., Kong, W., 2023. Ablation of the gut microbiota alleviates high-methionine diet-induced hyperhomocysteinemia and glucose intolerance in mice. *Npj Sci. Food* 7 (1). <https://doi.org/10.1038/s41538-023-00212-3>. Article 1.
- Li, X., Wei, T., Li, J., Yuan, Y., Wu, M., Chen, F., Deng, Z.-Y., Luo, T., 2022. Tyrosol ameliorates the symptoms of obesity, promotes adipose thermogenesis, and modulates the composition of gut microbiota in HFD fed mice. *Mol. Nutr. Food Res.* 66 (15), e2101015 <https://doi.org/10.1002/mnfr.202101015>.
- Li, X., Yao, Y., Wang, Y., Hua, L., Wu, M., Chen, F., Deng, Z.-Y., Luo, T., 2022. Effect of hesperidin supplementation on liver metabolomics and gut microbiota in a high-fat diet-induced NAFLD mice model. *J. Agric. Food Chem.* 70 (36), 11224–11235. <https://doi.org/10.1021/acs.jafc.2c02334>.
- Liu, T.-H., Wang, J., Zhang, C.-Y., Zhao, L., Sheng, Y.-Y., Tao, G.-S., Xue, Y.-Z., 2023. Gut microbial characteristic comparison reveals potential anti-aging function of *Dubosiella newyorkensis* in mice. *Front. Endocrinol.* 14, 1133167 <https://doi.org/10.3389/fendo.2023.1133167>.
- Liu, Y., Zhong, X., Lin, S., Xu, H., Liang, X., Wang, Y., Xu, J., Wang, K., Guo, X., Wang, J., Yu, M., Li, C., Xie, C., 2022. Limosilactobacillus reuteri and caffeoylquinic acid synergistically promote adipose browning and ameliorate obesity-associated disorders. *Microbiome* 10 (1), 226. <https://doi.org/10.1186/s40168-022-01430-9>.
- M, N., Pw, G., N, P., Lm, K., 2014. Role of the microbiome in energy regulation and metabolism. *Gastroenterology* 146 (6). <https://doi.org/10.1053/j.gastro.2014.02.008>.

- Ma, X., Xu, L., Alberobello, A.T., Gavriloa, O., Bagattin, A., Skarulis, M., Liu, J., Finkel, T., Mueller, E., 2015. Celastrol protects against obesity and metabolic dysfunction through activation of a HSF1-PGC1 α transcriptional Axis. *Cell Metabol.* 22 (4), 695–708. <https://doi.org/10.1016/j.cmet.2015.08.005>.
- MacLean, P.S., Higgins, J.A., Giles, E.D., Sherk, V.D., Jackman, M.R., 2015. The role for adipose tissue in weight regain after weight loss. *Obes. Rev.: Off J. Int. Associat. Stud. Obesit.* 16 (Suppl. 1), 45–54. <https://doi.org/10.1111/obr.12255>. Suppl 1.
- Mauvais-Jarvis, F., Arnold, A.P., Reue, K., 2017. A guide for the design of pre-clinical studies on sex differences in metabolism. *Cell Metabol.* 25 (6), 1216–1230. <https://doi.org/10.1016/j.cmet.2017.04.033>.
- Moreno-Navarrete, J.M., Fernandez-Real, J.M., 2019. The gut microbiota modulates both browning of white adipose tissue and the activity of brown adipose tissue. *Rev. Endocr. Metab. Disord.* 20 (4), 387–397. <https://doi.org/10.1007/s11154-019-09523-x>.
- Nierenberg, A.A., Ghaznavi, S.A., Sande Mathias, I., Ellard, K.K., Janos, J.A., Sylvia, L.G., 2018. Peroxisome proliferator-activated receptor gamma coactivator-1 alpha as a novel target for bipolar disorder and other neuropsychiatric disorders. *Biol. Psychiatr.* 83 (9), 761–769. <https://doi.org/10.1016/j.biopsych.2017.12.014>.
- Raja Kumar, S., Mohd Ramli, E.S., Abdul Nasir, N.A., Ismail, N.H.M., Mohd Fahami, N.A., 2019. Preventive Effect of Naringin on Metabolic Syndrome and its Mechanism of Action: A Systematic Review. Evidence-Based Complementary and Alternative Medicine. eCAM, 9752826. <https://doi.org/10.1155/2019/9752826>, 2019.
- Roopchand, D.E., Carmody, R.N., Kuhn, P., Moskal, K., Rojas-Silva, P., Turnbaugh, P.J., Raskin, I., 2015. Dietary polyphenols promote growth of the gut bacterium *akkermansia muciniphila* and attenuate high-fat diet-induced metabolic syndrome. *Diabetes* 64 (8), 2847–2858. <https://doi.org/10.2337/db14-1916>.
- Sang, T., Guo, C., Guo, D., Wu, J., Wang, Y., Wang, Y., Chen, J., Chen, C., Wu, K., Na, K., Li, K., Fang, L., Guo, C., Wang, X., 2021. Suppression of obesity and inflammation by polysaccharide from sporoderm-broken spore of *Ganoderma lucidum* via gut microbiota regulation. *Carbohydr. Polym.* 256, 117594 <https://doi.org/10.1016/j.carbpol.2020.117594>.
- Shelton, C.D., Sing, E., Mo, J., Shealy, N.G., Yoo, W., Thomas, J., Fitz, G.N., Castro, P.R., Hickman, T.T., Torres, T.P., Foegeding, N.J., Zieba, J.K., Calcutt, M.W., Codreanu, S. G., Sherrod, S.D., McLean, J.A., Peck, S.H., Yang, F., Markham, N.O., et al., 2023. An early-life microbiota metabolite protects against obesity by regulating intestinal lipid metabolism. *Cell Host Microbe* 31 (10), 1604–1619. <https://doi.org/10.1016/j.chom.2023.09.002> e10.
- Shi, X., Zhou, X., Chu, X., Wang, J., Xie, B., Ge, J., Guo, Y., Li, X., Yang, G., 2019. Allucin improves metabolism in high-fat diet-induced obese mice by modulating the gut microbiota. *Nutrients* 11 (12), 2909. <https://doi.org/10.3390/nu11122909>.
- Shin, J.-A., Lee, J.-H., Lim, S.-Y., Ha, H.-S., Kwon, H.-S., Park, Y.-M., Lee, W.-C., Kang, M.-I., Yim, H.-W., Yoon, K.-H., Son, H.-Y., 2013. Metabolic syndrome as a predictor of type 2 diabetes, and its clinical interpretations and usefulness. *J. Diabetes Investigat.* 4 (4), 334–343. <https://doi.org/10.1111/jdi.12075>.
- Sui, G.-G., Xiao, H.-B., Lu, X.-Y., Sun, Z.-L., 2018. Naringin activates AMPK resulting in altered expression of SREBPs, PCSK9, and LDLR to reduce body weight in obese C57bl/6J mice. *J. Agric. Food Chem.* 66 (34), 8983–8990. <https://doi.org/10.1021/acs.jafc.8b02696>.
- Thyagarajan, B., Foster, M.T., 2017. Beiging of white adipose tissue as a therapeutic strategy for weight loss in humans. *Horm. Mol. Biol. Clin. Invest.* 31 (2) <https://doi.org/10.1515/hmbci-2017-0016> j/hmbci.2017.31.issue-2/hmbci-2017-0016/hmbci-2017-0016.xml.
- Turnbaugh, P.J., Ley, R.E., Mahowald, M.A., Magrini, V., Mardis, E.R., Gordon, J.I., 2006. An obesity-associated gut microbiome with increased capacity for energy harvest. *Nature* 444 (7122), 1027–1031. <https://doi.org/10.1038/nature05414>.
- Ussar, S., Griffin, N.W., Bezy, O., Fujisaka, S., Vienberg, S., Softic, S., Deng, L., Bry, L., Gordon, J.I., Kahn, C.R., 2015. Interactions between gut microbiota, host genetics and diet modulate the predisposition to obesity and metabolic syndrome. *Cell Metabol.* 22 (3), 516–530. <https://doi.org/10.1016/j.cmet.2015.07.007>.
- Vitali, A., Murano, I., Zingaretti, M.C., Frontini, A., Ricquier, D., Cinti, S., 2012. The adipose organ of obesity-prone C57BL/6J mice is composed of mixed white and brown adipocytes. *JLR (J. Lipid Res.)* 53 (4), 619–629. <https://doi.org/10.1194/jlr.M018846>.
- Wang, L., Jin, G., Yu, C., Lv, J., Guo, Y., Bian, Z., Yang, L., Chen, Y., Hu, Z., Chen, F., Chen, Z., Li, L., Shen, H., China Kadoorie Biobank Collaborative Group, 2020. Cancer incidence in relation to body fatness among 0.5 million men and women: findings from the China Kadoorie Biobank. *Int. J. Cancer* 146 (4), 987–998. <https://doi.org/10.1002/ijc.32394>.
- Wolfrum, C., Gerhart-Hines, Z., 2022. Fueling the fire of adipose thermogenesis. *Science (New York, N.Y.)* 375 (6586), 1229–1231. <https://doi.org/10.1126/science.abl7108>.
- X, Z., Qx, Z., X, W., L, Z., W, Q., B, B., Ca, L., J, L., 2016. Dietary luteolin activates browning and thermogenesis in mice through an AMPK/PGC1 α pathway-mediated mechanism. *Int. J. Obes.* 40 (12) <https://doi.org/10.1038/ijo.2016.108>, 2005.
- Xing, T., Kang, Y., Xu, X., Wang, B., Du, M., Zhu, M.-J., 2018. Raspberry supplementation improves insulin signaling and promotes Brown-like adipocyte development in white adipose tissue of obese mice. *Mol. Nutr. Food Res.* 62 (5) <https://doi.org/10.1002/mnfr.201701035>.
- Yang, K., Jian, S., Guo, D., Wen, C., Xin, Z., Zhang, L., Kuang, T., Wen, J., Yin, Y., Deng, B., 2022. Fecal microbiota and metabolomics revealed the effect of long-term consumption of gallic acid on canine lipid metabolism and gut health. *Food Chem. X* 15, 100377. <https://doi.org/10.1016/j.fochx.2022.100377>.
- Yuan, T., Li, J., Zhao, W.-G., Sun, W., Liu, S.-N., Liu, Q., Fu, Y., Shen, Z.-F., 2019. Effects of metformin on metabolism of white and brown adipose tissue in obese C57BL/6J mice. *Diabetol. Metab. Syndrome* 11, 96. <https://doi.org/10.1186/s13098-019-0490-2>.
- Zeng, S.-L., Li, S.-Z., Xiao, P.-T., Cai, Y.-Y., Chu, C., Chen, B.-Z., Li, P., Li, J., Liu, E.-H., 2020. Citrus polymethoxyflavones attenuate metabolic syndrome by regulating gut microbiome and amino acid metabolism. *Sci. Adv.* 6 (1), eaax6208 <https://doi.org/10.1126/sciadv.aax6208>.
- Zhao, M., Wang, B., Li, L., Zhao, W., 2023. Anti-obesity effects of dietary fibers extracted from flaxseed cake in diet-induced obese mice. *Nutrients* 15 (7), 1718. <https://doi.org/10.3390/nu15071718>.